Conformational Preference of Macrocycles Investigated by Ion-Mobility Mass Spectrometry and Distance Geometry Modeling

Authors: Isaac W. Haynes,[+⊥] Guangcheng Wu,[#⊥] MD Ashraful Haque,[+] Hao Li,[#] * Thanh D. Do[+]*

[+]Department of Chemistry, University of Tennessee, Knoxville TN 37996, USA

[#] Department of Chemistry, Zhejiang University, Hangzhou 310027, China

Email: tdo5@utk.edu, lihao2015@zju.edu.cn

[⊥]I.W.H. and G.W. contributed equally to this work.

Supporting Information

Table of Content.

Synthesis of macrocycles MA_n. A 1:1 mixture of $\mathbf{A}^{2+}\bullet 2Br^-$ (115.6 mg, 0.20 mmol) and the corresponding bishydrazide linkers **H-n** (n = 4 to 7) (0.20 mmol) were dissolved in 100 mL water. An aliquot of 8-µL TFA was added to catalyze the reaction. The corresponding reaction mixtures were stirred over night at 50°C. After cooling to room temperature, the solutions were filtered to remove insoluble byproducts. 0.6 g of $NH_4^+\bullet PF_6^-$ was added into the filtrate with stirring, yielding $MA_n^{2+}\bullet 2PF_6^-$ as yellow precipitates. ^{1}H-NMR spectra (CD_3CN, 500M) of $MA_n^{2+}\bullet 2PF_6^-$ are consistent with published literature.[1]

In the acetonitrile solutions of $MA_n^{2+}\bullet 2PF_6^-$ was added to an excess amount of $Bu_4N^+\bullet Cl^-$, and to yield pale yellow precipitates. These precipitates were collected by filtration and washed with acetonitrile, yielding $MA_n^{2+}\bullet 2Cl^-$ as a pale-yellow powder. ^{1}H-NMR spectra (D_2O, 500M) of $MA_n^{2+}\bullet 2Cl^-$ are also consistent with published literature.[1]

IMS-MS Methods. All mobility data were obtained by step-field method using ΔV = 889.60, 790.00, 690.00, 589.60 and 490.50. Upon exiting the drift cell, the ions were focused by an exit funnel into a QTOF mass analyzer. Arrival time distributions were extracted using IM-MS Browser B.07.01 and processed with Origin Pro 2018b. The arrival time t_A is related to ΔV by Eq. 1.[2]

$$t_A = \frac{L^2\ T_0\ \ P}{K_0 P_0 T \Delta V} + t_0 \quad \text{(Eq. 1)}$$

where L is the length of the drift tube (L = 78.1 cm), K_0 is the reduced mobility, P and T are the buffer gas pressure and temperature, respectively. T_0 = 273.15 K and P_0 = 760 Torr. The CCS can be calculated from K_0 using Eq. 2.[2]

$$\sigma_{exp} \approx \frac{3ze}{16N_0}\sqrt{\frac{2\pi}{\mu k_B T}}\frac{1}{K_0} \quad \text{(Eq. 2)}$$

LC-IMS-MS Methods. For LC separations by LC–IMS-QTOF, 1.5 µl of the sample was loaded onto a ZORBAX Extend-C18 (5 µm; Agilent; part 773700-902). The sample was separated using a gradient elution with the following conditions: solvent A 99.9% H_2O, 0.1% FA; solvent B 100% ACN, flow rate 200 µl/min, temperature 40 °C, gradient 0–3 min, 2% B; 3–5 min, 2–20% B; 5–18 min, 20–35% B; 18–23 min, 35-50% B; 23-26 min, 50– 95% B; 26–27 min, 95% B; 27–30 min, 95-2% B.

Table S1. Tuning parameters (positive polarity) used in this work.

Parameter	Value
Pre-IMS Zone	
Source: gas temperature	300 °C
Source: drying gas	5 l/min
Source: nebulizer pressure	13 psi
Source: capillary	3500 V
Optics I: fragmentor	250 V
IM front funnel: high pressure funnel delta	110 V
IM front funnel: high pressure RF delta	180 V
IM front funnel: trap funnel delta	160 V
IM front funnel: trap funnel RF	180 V
IM front funnel: trap funnel exit	10 V
IM trap: trap entrance grid low	82 V
IM trap: trap entrance grid delta	2 V
IM trap: trap entrance	79 V
IM trap: trap exit	76 V
IM trap: trap exit grid 1 low	72 V
IM trap: trap exit grid 1 delta	6 V
IM trap: trap exit grid 2 low	71 V
IM trap: trap exit grid 2 delta	13 V
Acquisition: trap fill time	1000 µs
Acquisition: trap release time	100 µs
Post-IMS Zone	
IM drift tube: drift tube exit	210 V
IM rear funnel: rear funnel entrance	200 V
IM rear funnel: rear funnel RF	130 V
IM rear funnel: rear funnel exit	35 V
IM rear funnel: IM Hex entrance	42 V
IM rear funnel: IM Hex delta	8
Optics 1: Oct entrance lens	32 V
Optics 1: Lens 1	28.3 V
Optics 1: Lens 2	15.8 V
Quad: Quad DC	26.6 V
Quad: postfilter DC	26.5 V
Cell: gas flow	22 psi
Cell: cell entrance	25.6 V
Cell: Hex DC	24.2 V
Cell: Hex delta	-9 V
Cell: Hex2 DC	15 V
Cell: Hex2 DV	-3 V
Optics 2: Hex3 DC	11.8 V
Extractor: ion focus	5.6 V

Table S2. Monomer and Dimer CCSs of $MA_n^{2+}•2Cl^-$ in water.

Macrocycle	*m/z*	Species	CCS
$MA_4^{2+}•2Cl^-$	278	$[MA_4^{2+}]$	178
	555	$[MA_4^{1+}]$	156
			167
		$2[MA_4^{1+}]$	263
	591	$[MA_4^{2+}•Cl^-]$	168
		$2[MA_4^{2+}•Cl^-]$	252
			259
$MA_5^{2+}•2Cl^-$	285	$[MA_5^{2+}]$	183
	569	$[MA_5^{1+}]$	161
			170
		$2[MA_5^{1+}]$	268
	605	$[MA_5^{2+}•Cl^-]$	162
			169
		$2[MA_5^{2+}•Cl^-]$	245
			269
$MA_6^{2+}•2Cl^-$	292	$[MA_6^{2+}]$	185
	583	$[MA_6^{1+}]$	164
		$2[MA_6^{1+}]$	264
	619	$[MA_6^{2+}•Cl^-]$	172
		$2[MA_6^{2+}•Cl^-]$	276
$MA_7^{2+}•2Cl^-$	299	$[MA_7^{2+}]$	192
	597	$[MA_7^{1+}]$	171
		$2[MA_7^{1+}]$	263
			276
	633	$[MA_7^{2+}•Cl^-]$	173
		$2[MA_7^{2+}•Cl^-]$	265
			279

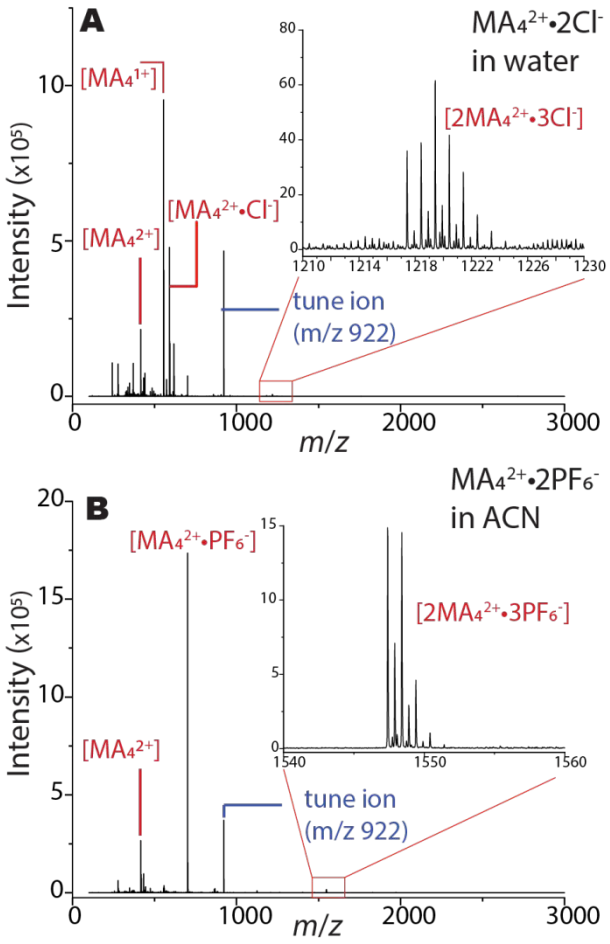

Figure S1. ESI/Jet Stream mass spectra of MA_4^{2+}•Cl^- and MA_4^{2+}•PF_6^- in (A) water and (B) acetonitrile (ACN), respectively. The analyte concentration is 10-20 µM. Major mass spectral peaks are annotated.

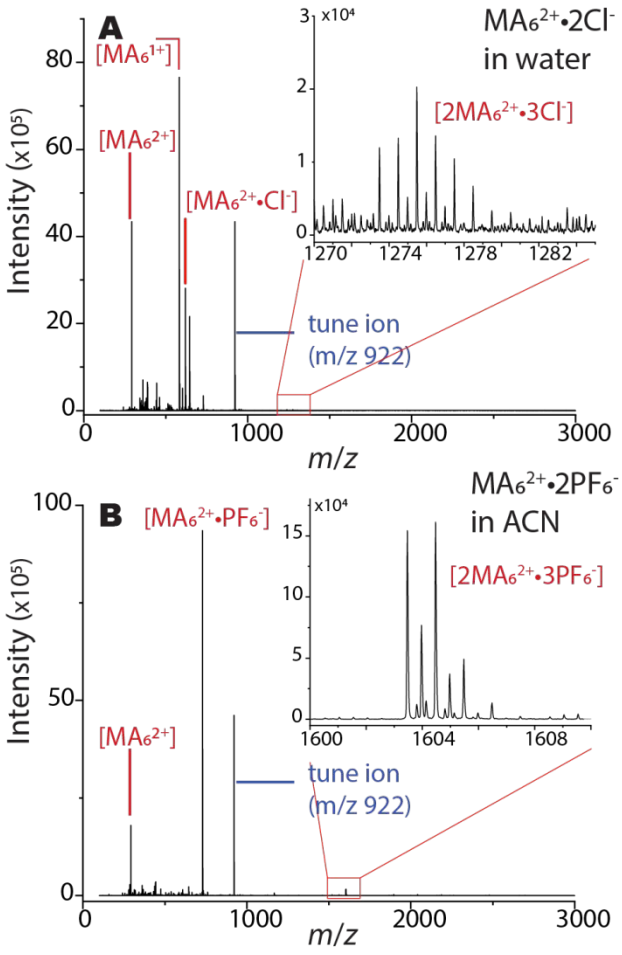

Figure S2. ESI/Jet Stream mass spectra of MA_6^{2+}•Cl^- and MA_6^{2+}•PF_6^- in (A) water and (B) acetonitrile (ACN), respectively. The analyte concentration is 10-20 µM. Major mass spectral peaks are annotated.

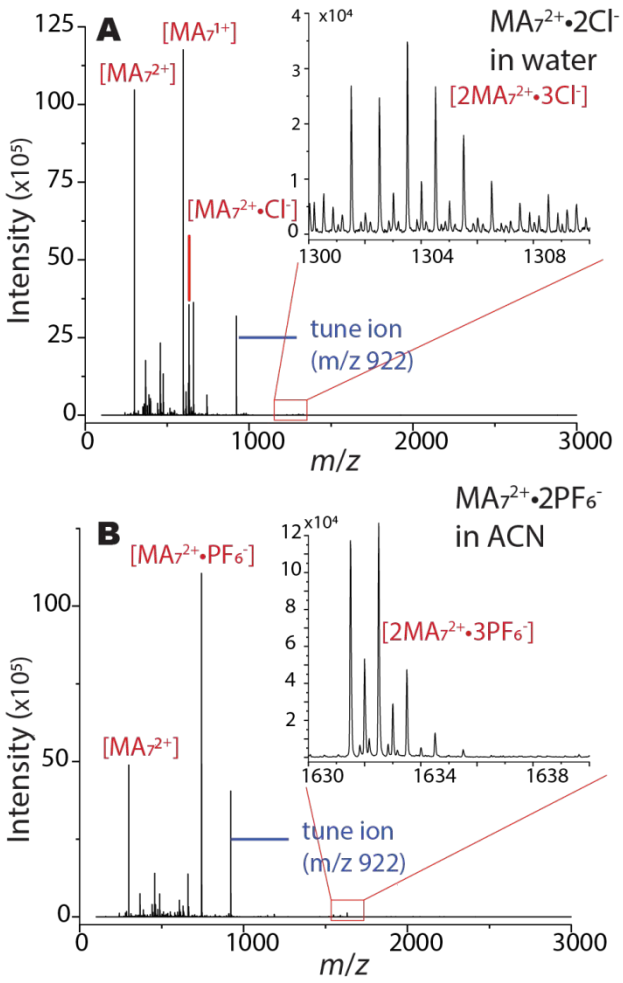

Figure S3. ESI/Jet Stream mass spectra of MA_7^{2+}•Cl^- and MA_7^{2+}•PF_6^- in (A) water and (B) acetonitrile (ACN), respectively. The analyte concentration is 10-20 μM. Major mass spectral peaks are annotated.

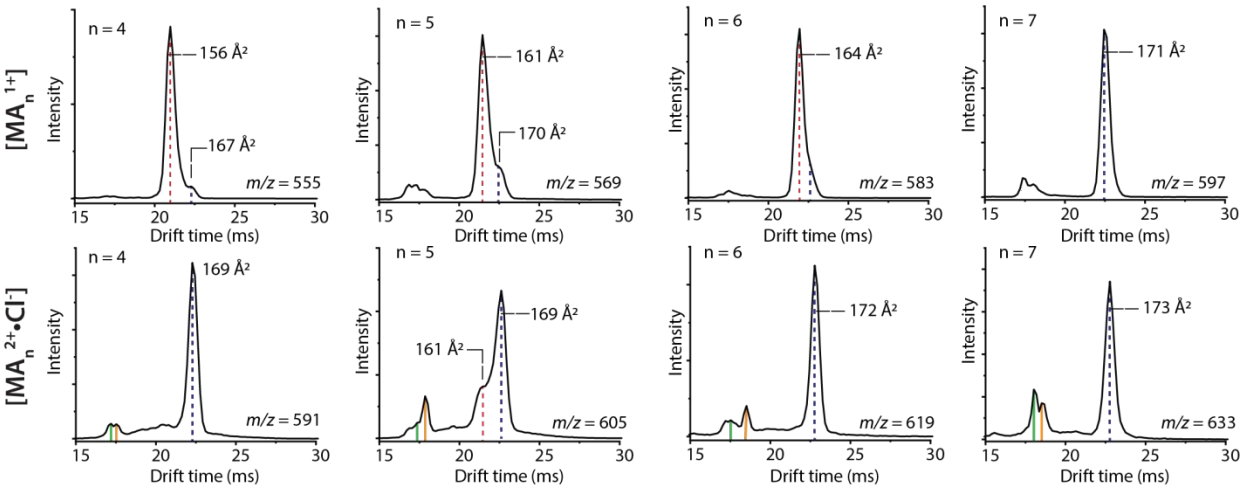

Figure S4. Representative ATDs of $[MA_n^{1+}]$ and $[MA_n^{2+}•Cl^-]$ (n = 4, 5, 6, 7). Conformations I and II are annotated by dashed lines in blue and red, respectively. Macrocycle clusters and catenanes are also detected at shorter drift times labeled by green and orange vertical lines.

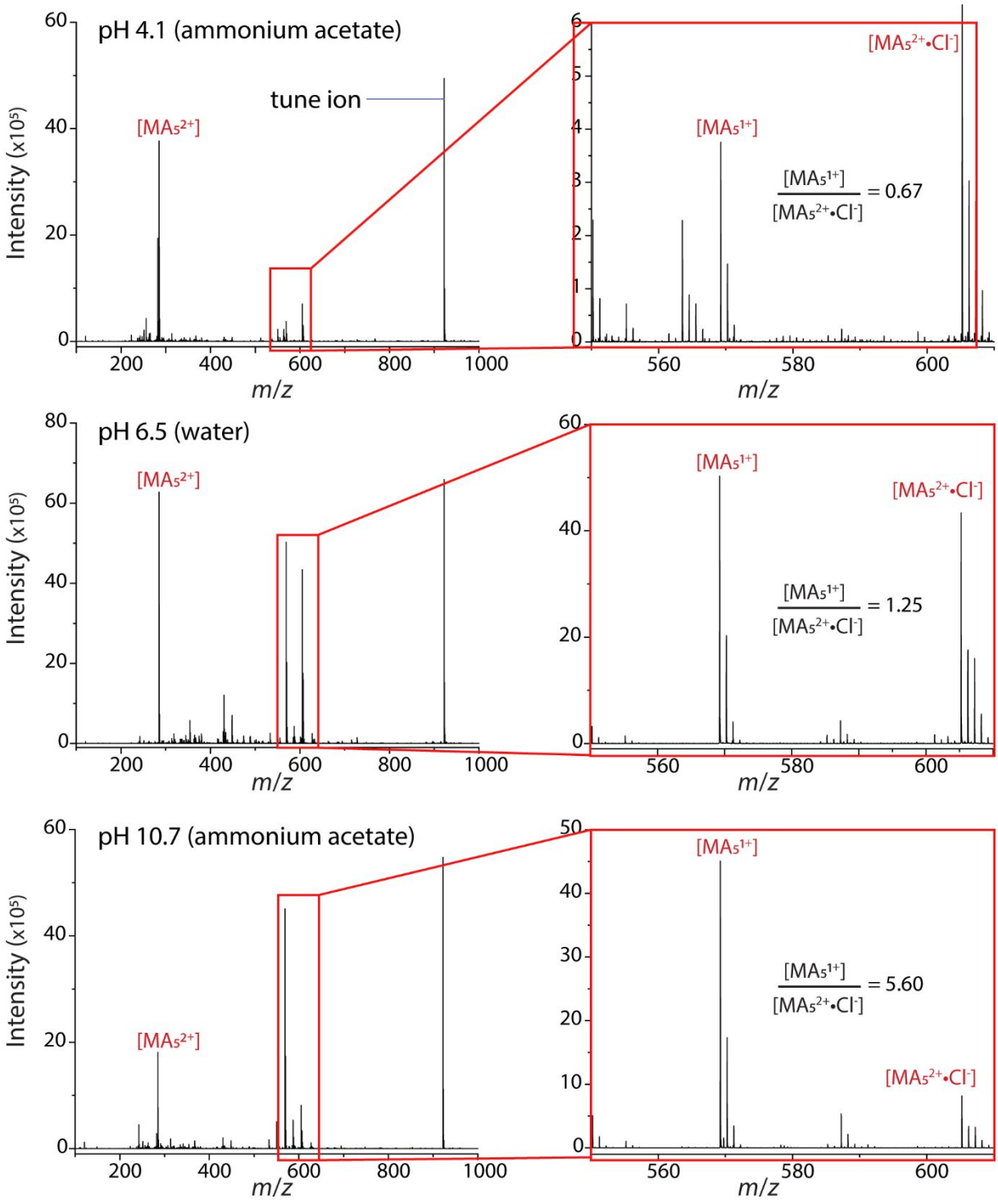

Figure S5. Representative mass spectra of $[MA_5^{2+}\bullet Cl^-]$ at pH = 4.1, 6.5 and 10.7.

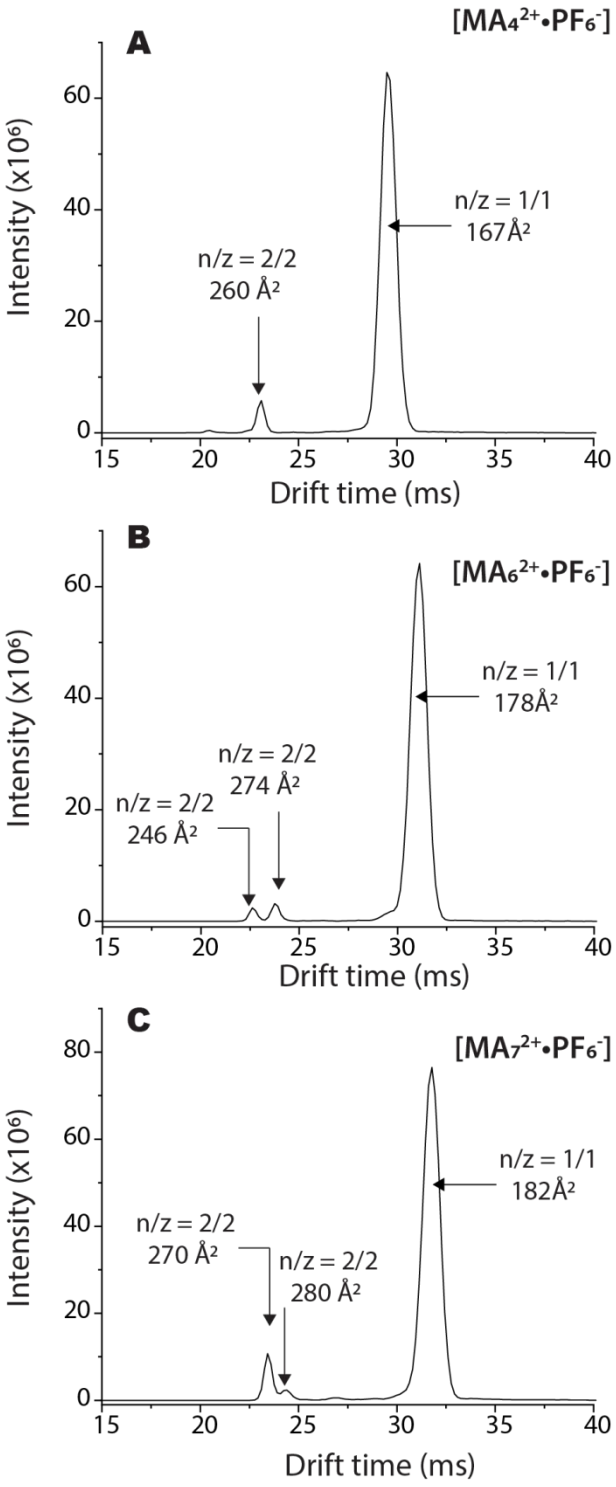

Figure S6. Representative ATDs of $[MA_n^{2+}•PF_6^-]$ (A) $n = 4$, (B) $n = 6$ and (C) $n = 7$.

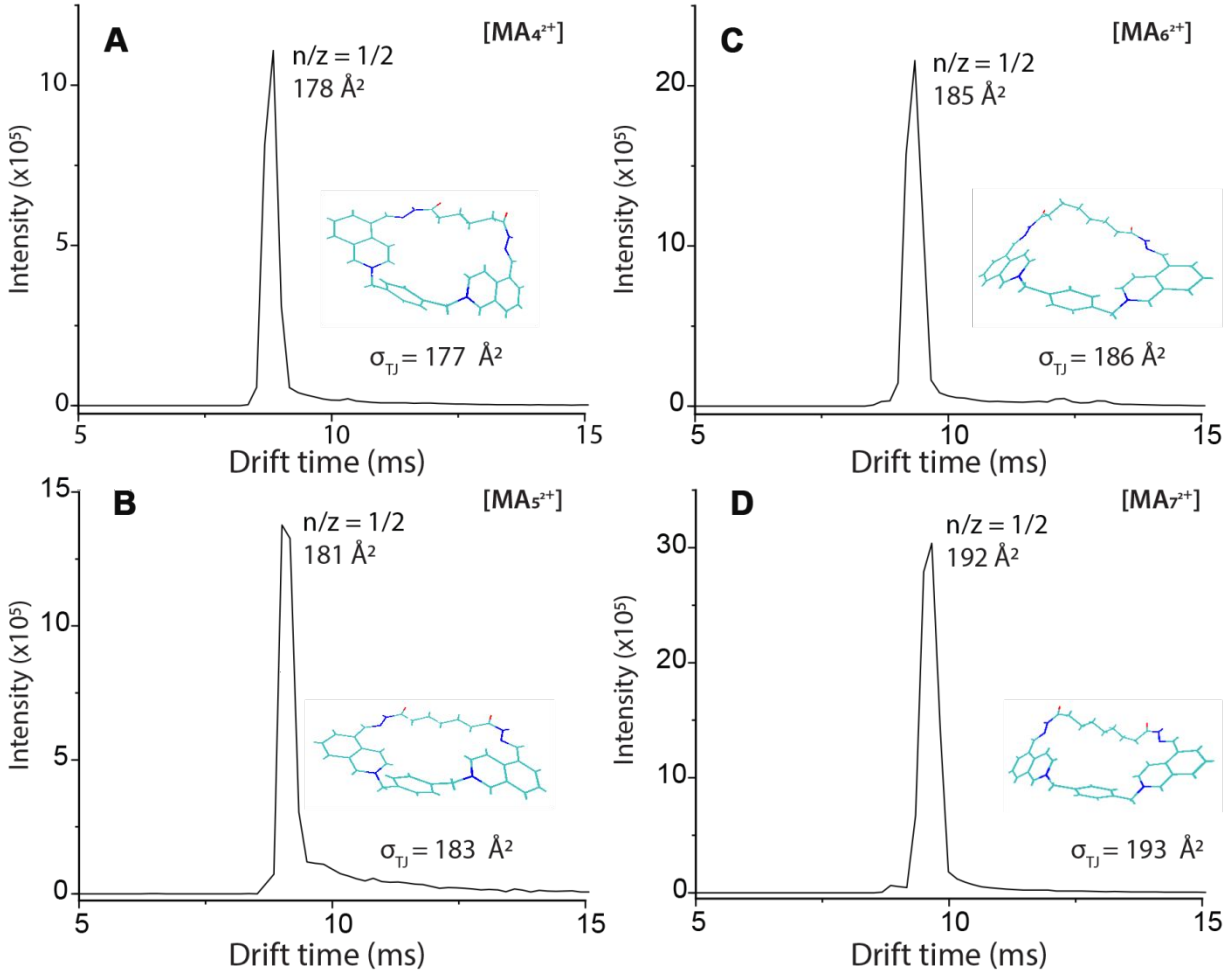

Figure S7. Representative ATDs of $[MA_n^{2+}]$. (A) $[MA_4^{2+}]$ at *m/z* 278, (B) $[MA_5^{2+}]$ at *m/z* 285, (C) $[MA_6^{2+}]$ at *m/z* 292 and (D) $[MA_7^{2+}]$ at *m/z* 299. DG model structures (see main text) and theoretical CCS are also shown.

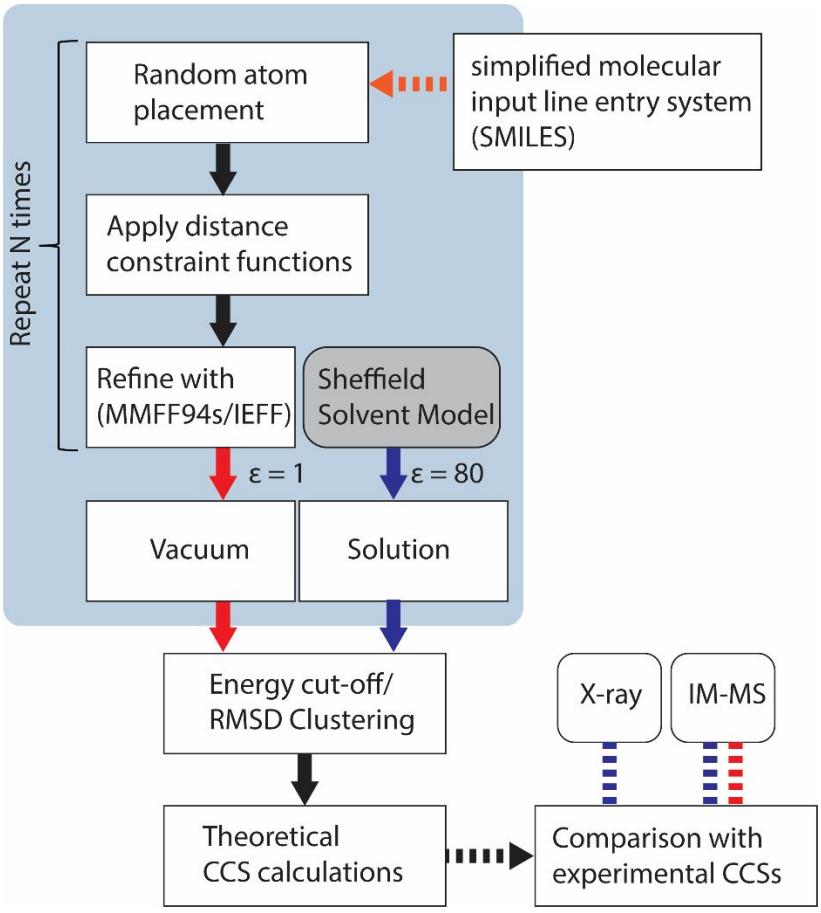

Figure S8. Distance geometry modeling workflow.

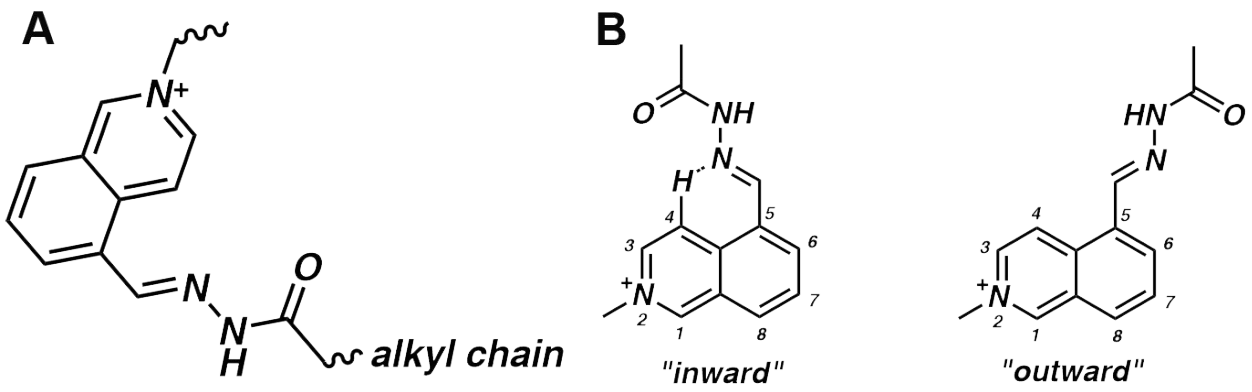

Figure S9. (A) The C(H)-N-N(H)-C(O)-C(alkyl chain) adopts a zigzag shape, (B) Comparison between "inward" and "outward" orientations of the imine nitrogen for the E-rotational isomer. The hydrogen bond is formed between the hydrogen of isoquinoline C4 and the "inward" imine.

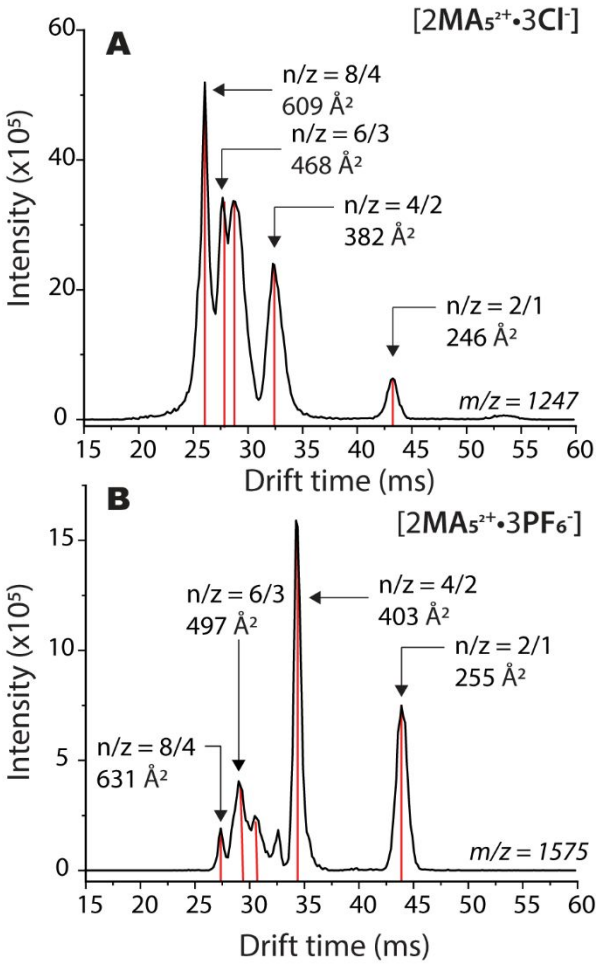

Figure S10. Representative ATDs of (A) $[2MA_5^{2+}•3Cl^-]$ in water and (B) $[2MA_5^{2+}•PF_6^-]$ in ACN.

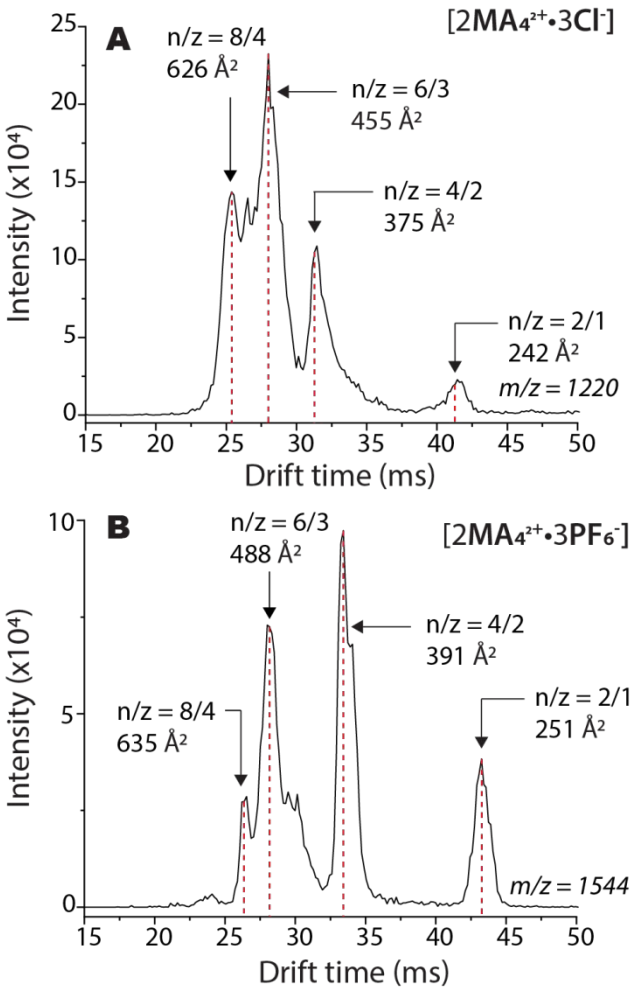

Figure S11. Representative ATDs of (A) $[2MA_4^{2+}•3Cl^-]$ in water and (B) $[2MA_4^{2+}•PF_6^-]$ in ACN.

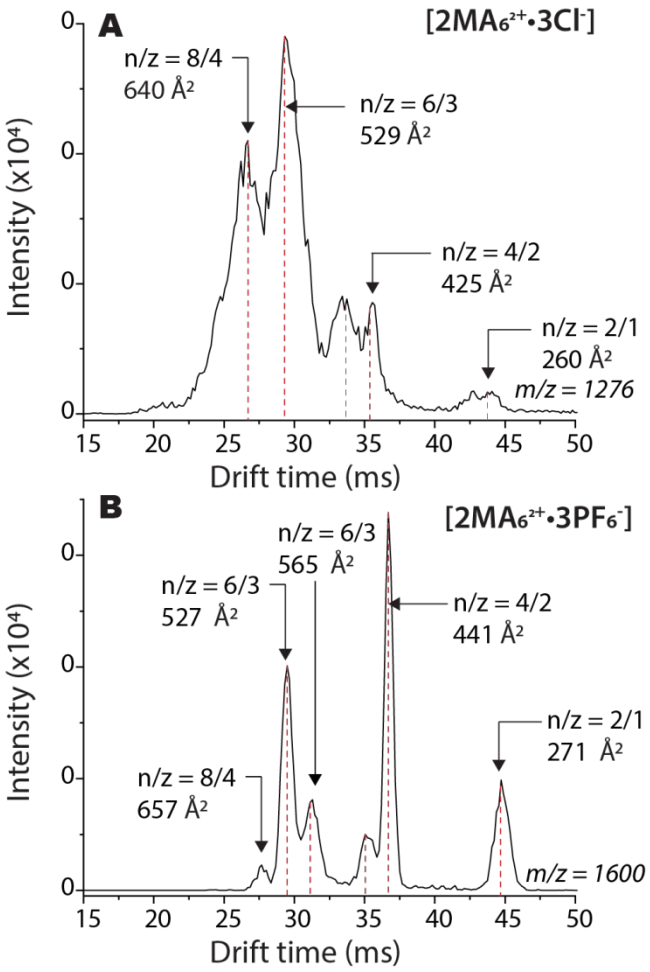

Figure S12. Representative ATDs of (A) $2MA_6^{2+}•3Cl^-$ in water and (B) $2MA_6^{2+}•3PF_6^-$ in ACN.

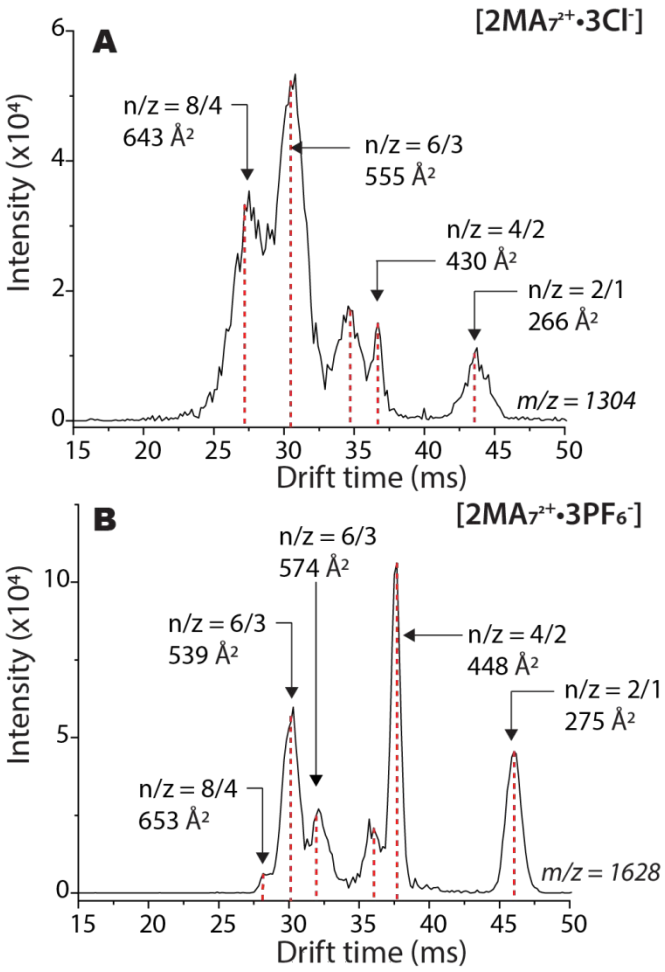

Figure S13. Representative ATDs of (A) $2MA_7^{2+}•3Cl^-$ in water and (B) $2MA_7^{2+}•3PF_6^-$ in ACN.

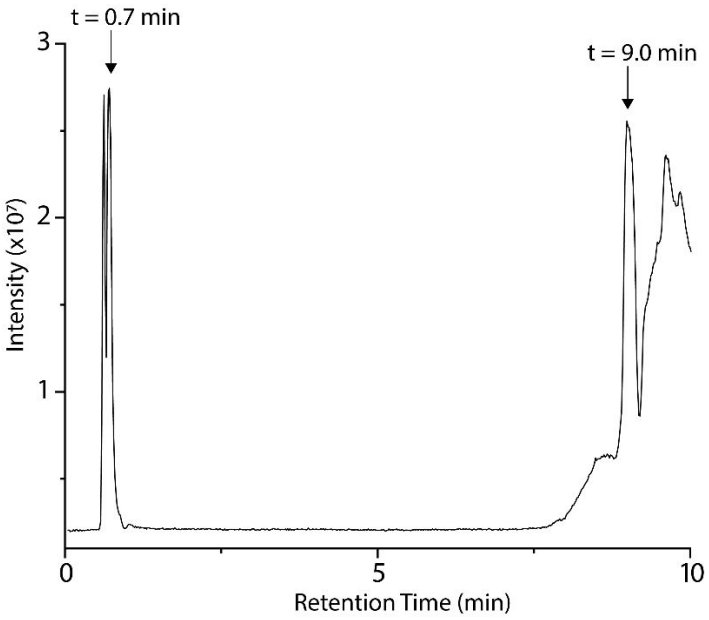

Figure S14. LC chromatogram of 100 μM MA_5^{2+}•2Cl^-.

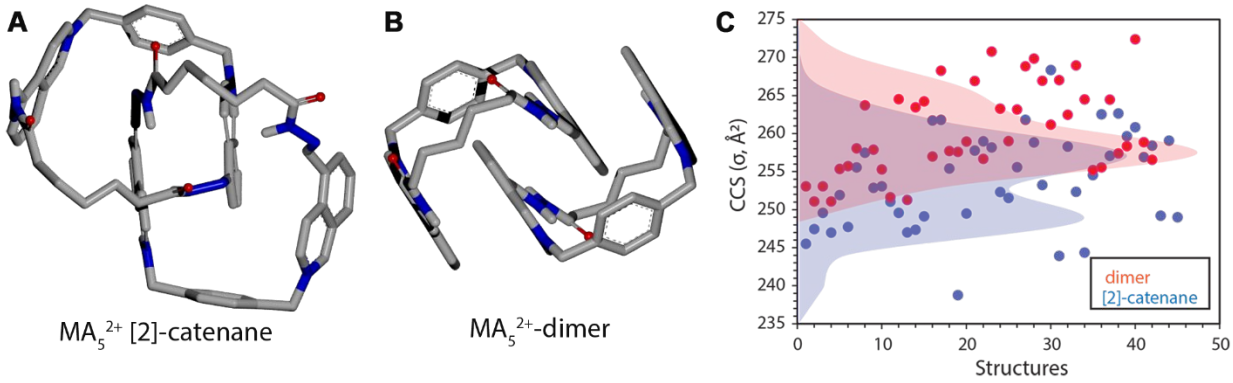

Figure S15. (A-B) Model structures of [2]-catenane and dimer of MA_5^{2+}. (C) Theoretical CCS distributions of model structures.

References Cited.

1. Wu, G.; Wang, C. Y.; Jiao, T.; Zhu, H.; Huang, F.; Li, H., *J Am Chem Soc* **2018,** *140* (18), 5955-5961.

2. Mason, E. A.; McDaniel, E. W., *Transport Properties of Ions in Gases*. 99 ed.; Wiley-VCH: New York, 1988.